Autocorrelation Statistics-Based Algorithms for Automatic Ground and Non-ground Classification of Lidar Data

Sara Shirowzhan[a] and Samsung Lim[b]

[a,b] School of Civil and Environmental Engineering, University of New South Wales, Australia
E-mail: S.Shirowzhan@student.unsw.edu.au, S.lim@unsw.edu.au

Abstract –

Classification of lidar data to ground and non-ground points is important for accurate topography mapping and reliable estimation of slope, volume and buildings' geometry over urban areas. Manual or semi-automatic classification provides relatively good results, however, automatic classification in complex areas with diverse object sizes is still challenging.

This research aims to propose two novel algorithms based on Getis-Ord *Gi (or *Gi** for short) and Local Moran's *I* (LMI) statistics to classify a lidar point cloud into a set of points representing ground and another set of points reflected from non-ground e.g. buildings and vegetation. The**

Two statistics, *Gi and LMI, have been widely used in cluster analysis to identify clustered features of high *z*-scores and low *z*-scores. Based on the two statistics, we proposed two classification algorithms that allow varying window sizes e.g. 100 m, 150 m and 200 m, and applied the algorithms to the lidar data in order to obtain optimal classification results. The results show that the *Gi**-based algorithm decreases omission errors but increases commission errors when compared to the LMI-based approach. Overall the 100-m window size outperforms than the other window sizes in terms of feature extraction in slant areas, whereas the 150-m window size provides slightly better results in a complex scene of high-rise buildings and dense vegetation, and the 200-m window size is more efficient if large buildings are present in the study area. This feasibility study indicates that autocorrelation statistics such as *Gi** and LMI can be effectively used to classify a lidar point cloud.**

Keywords -

Automatic classification, Bare earth extraction, Spatial association, DSM, DEM, NDSM

1 Introduction

A Digital Elevation Model (DEM) is a grid containing elevation information of ground which can be derived from lidar point clouds. The DEM can be used for topography mapping and extraction of non-ground points including man-made and natural objects such as buildings and trees. Light detection and ranging (lidar) is a proven technology for generating highly accurate Digital Elevation Models (DEMs). However, Pingel et al. [1] reported that terrain classification is a challenging problem for DEM production since classification errors, commission errors in particular, are always inevitable.

Although conventional filtering algorithms e.g. morphological filters for classification in general areas are performing well, accurate classification of lidar point clouds in complex urban scenes including large and small objects with diverse elevation [2-4] is challenging. Classification results often depend on the assumptions made to the neighbours of each lidar point [5]. One of the assumptions is that the points representing an artificial object are clustered with elevations above the mean value of the neighbours, and the points representing ground are also clustered but have elevations below the mean value [6]. This assumption can be formulated as a criterion for lidar data classification by utilising some spatial autocorrelation statistics. For example, Getis and Ord [7] claimed that using Moran's *I* (MI) in conjunction with the *G* statistic would improve the understanding of a given spatial data set. Hence this study aims to apply two local statistics, namely, Local Moran's *I* (LMI) and Getis-Ord G_i* (or G_i* for short), for effective classifications of a lidar point cloud into points representing ground and points reflected from non-ground such as buildings and vegetation.

Previously, MI has been applied to images as a texture measurement tool for object classification [8-11]. Su et al. [10] claimed that a higher accuracy for object classification is achieved by applying MI, compared to other spectral and textural measurement methods. They achieved 87% of Cohen's kappa index as an accuracy indicator of the MI-based classification. However, the calculation of MI for lidar data is challenging because of the high point density. On the other hand, LMI is one of the spatial autocorrelation statistics that Roggero [12] utilised for deriving information from spectral images. The potential of LMI comes from the nature of its spatial autocorrelation functionality that compares a local variation with the global variation [12, p. 58]. In this paper, a local variation of elevation is compared with the overall variance of elevation in a pre-defined window.

The Global Moran's I (GMI) is defined by [13] as follows:

$$I = \frac{N\sum_i\sum_j W_{i,j}Z_iZ_j}{\sum_i Z_i^2} \quad (1)$$

$$\sum_i\sum_j W_{i,j} = 1 \quad (2)$$

where Z_i and Z_j refer to the deviation of attribute values (i.e. elevation information of the lidar points in this study) of features i and j from the mean value within the distance threshold of a neighborhood and N is the total number of features within the neighborhood. In addition, $W_{i,j}$'s are spatial weights between the pairs i and j e.g. inversed distance weights between the pairs. While GMI as a spatial autocorrelation shows the overall similarities or dissimilarities, LMI is known as a more effective spatial autocorrelation indicator which can be used for a microscopic analysis of GMI. Indeed, LMI exhibits the contribution from each observation to the global indicator [13]. From Equation (1), Anselin [13] defined LMI as:

$$I_i = Z_i\sum_j W_{i,j}Z_j \quad (3)$$

where the weight was conveniently allocated as the inverse distance between the features i and j.

A positive LMI indicates that the lidar point belongs to a cluster of similar values, and a negative LMI indicates that the lidar point is dissimilar to the neighbours. As LMI depends strongly on the neighbours, it is a relative measure [14] and therefore cannot be regarded as a z-score for lidar point classification. According to [15], the z-score of LMI is defined as follows.

$$z_i = \frac{I_i - E[I]}{\sqrt{V[I_i]}} \quad (4)$$

where E and V represent the expected mean and variance, respectively.

All classification algorithms suffer from two types of errors: Type 1 errors (i.e. omission errors), and Type 2 errors (i.e. commission errors) [5]. In this paper we argue that, when it comes to ground-point classification, omission errors are not so critical for deriving a DEM as long as commission errors remain small because the DEM is interpolated from the correctly classified ground points. Consequently, omission errors for non-ground points can be less important in an initial classification step because the non-ground points can be reclassified by applying the DEM. For this reason, the main aim of this study is to minimize commission errors, even though omission errors will be assessed as well. G_i* can be defined as [16]:

$$G_i^* = \frac{\sum_j W_{i,j}Z_j - E[Z]}{\sqrt{V[Z]\frac{N\sum_j W_{i,j}^2 - 1}{N-1}}}. \quad (5)$$

The meaning of a significance level of G_i* and LMI was explained by Getis and Ord [7]. That is, clusters of high or low values are obtained by choosing a significant LMI z-score. In general, a significant z-score is chosen to be higher than 2.58 or lower than -2.58 where the corresponding p-value is smaller than 0.05. As for the significance level of z-scores, Ebdon stated that "The probability that the null hypothesis is correct is referred as the significance level. The null hypothesis can be rejected if this probability is acceptably low. Significance levels of 0.05 or even 0.1 are possibly adequate in many geographical applications" [17, p.16].

In this paper, two significant levels of the LMI z-scores and G_i* values are used for lidar point classification because it is observed that significant positive values are obtained in the clusters of high-elevation lidar points and significant negative values are found in the clusters of low-elevation lidar points. The significance level of the LMI z-scores is ±2.58, that is, ground points are supposed to have z-scores less than -2.58, and non-ground points have z-scores greater than 2.58. However, the significance level of G_i* is chosen differently in order to improve the classification results, that is, less than -1.65 for ground, or greater than 1.65 for non-ground. This paper presents and tests the two algorithms based on the statistics of G_i* and LMI, then discusses advantages and disadvantages of the two algorithms by investigating omission errors and commission errors.

2 Methodology

In this study we use the lidar data set over the University of New South Wales (UNSW) with 20-cm horizontal accuracy and 12-cm vertical accuracy. The study extent is illustrated in Figure 1.

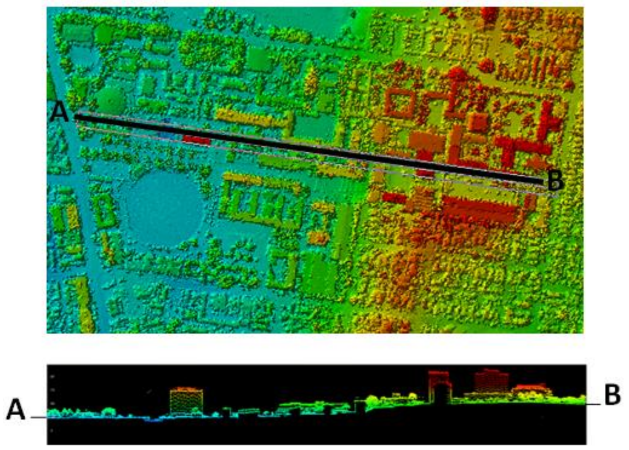

Figure 1. Study extent and the vertical profile along the line segment between Point A and Point B.

As can be seen in Figure 1, the study extent consists of flat and slant areas, small and large objects with various elevation values (see the vertical profile along the line segment between Point A and Point B in Figure 1). The study area contains 2 challenging areas for object classification: a steep slope area and a complex area. The complex area includes high-rise buildings, large-size buildings, and tall trees. In this study two algorithms are proposed: one based on LMI and the other based on G_i*. With the two algorithms, three different window sizes of 100 m, 150 m and 200 m are tested. For each window size, ground and non-ground points are classified by applying the two algorithms. The G_i* -based algorithm is defined as:

1. *Set a window size. For each window,*
2. *Calculate G_i* with a pre-defined neighbourhood and weights*
3. *Assign the clusters of low values (G_i* < -1.65 and p-value < 0.05) to ground*
4. *Assign the clusters of high values (G_i* > 1.65 and p-value < 0.05) to non-ground*
5. *Verify the results against the reference*.

The LMI-based algorithm is similar to the G_i* -based except that the LMI *z*-score is used instead of G_i*, and the significance level is ±2.58 instead of ±1.65. Test results of ground and non-ground classification using the proposed algorithms will be compared to the reference ground and the reference non-ground, respectively. Two datasets of ground and non-ground shown in Figures 2a and 2b, respectively, are the classification results from a commercial software package known as Terrasolid, which can be used as a reference for comparison purposes as they are independently obtained. Low vegetation is outside our study scope, hence points of less than 1-m height are removed from non-ground data. Low vegetation thresholds of 0.5, 1, 1.5, 2 and 2.5 m were tested by Estornell et al. [18] who concluded that the larger the thresholds they chose, the smaller error levels they obtained. In our case, any thresholds greater than 1 m are not appropriate because substantial vegetation of 1-m height or higher were observed in the study area.

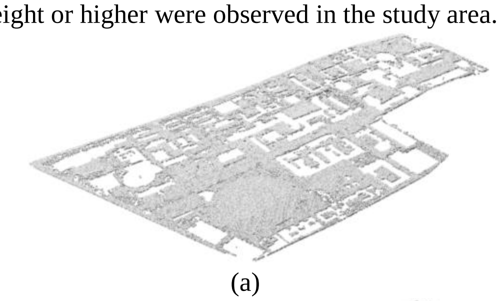

(a)

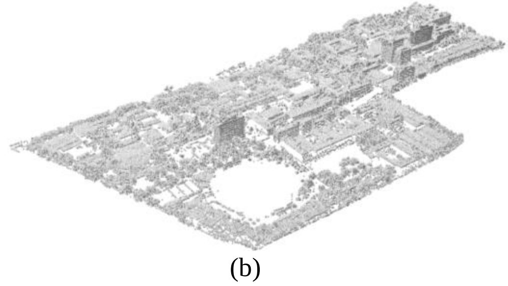

(b)

Figure 2. Oblique view of reference points: (a) ground, (b) non-ground.

3 Validation

For validation of the results, two types of errors are calculated: Type 1 errors and Type 2 errors. Type 1 occurs when the algorithm "rejects the null hypothesis even though it is true" and Type 2 occurs when the algorithm "fails to reject the null hypothesis even though it is false" [19, p. 147]. Our null hypothesis for lidar data classification is that ground points have low *z*-scores and non-ground points have high *z*-scores. Therefore, Type 1 in ground classification occurs when the lidar point is actually reflected from ground but is not classified as a ground point, hence it belongs to an omission error. Type 2 in ground classification occurs when the lidar point is reflected from non-ground e.g. a building or a tree but is classified as a ground point i.e. it can be categorized as a commission error. Omission errors and commission errors in non-ground classification can be defined similarly.

4 Results

One of the objectives of this paper is to show that, by applying G_i* and MI, clusters of low *z*-scores can be identified from ground points and clusters of high *z*-scores can be identified from non-ground points. Figures 3a and 3b show the extracted ground and non-ground points from the LMI-based algorithm using window sizes of 100 m, 150 m and 200 m. Comparing reference ground points (Figure 2a) and ground points extracted by the LMI-based algorithm (Figure 3a), it shows that a slant area is the subject of commission error (i.e. non-ground points are classified as ground points). On the other hand, low vegetation and man-made objects are the main areas of omission error in non-ground points.

(a)

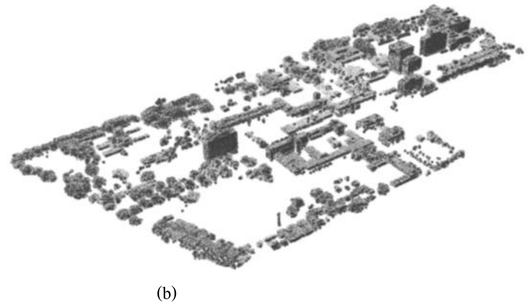

(b)

Figure 3. Combined results of 100-m, 150-m and 200-m window sizes: (a) ground and (b) non-ground, using the LMI-based algorithm,

Figures 4a and 4b show the all extracted ground and non-ground points with 100-m, 150-m and 200-m window sizes using the *Gi**-based algorithm. Comparison of the overall results from the LMI-based algorithm and the *Gi**-based algorithm with reference ground and non-ground points indicates that the level of commission error increases while the level of omission error decreases. This is confirmed if we compare Tables 1 and 2.

(a)

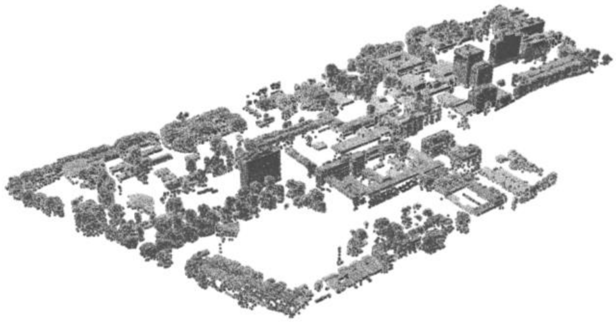

(b)

Figure 4. Combined results of 100-m, 150-m and 200-m window sizes: (a) ground and (b) non-ground, using the G_i* -based algorithm

The results from the LMI-based algorithm and the G_i* -based algorithm are demonstrated in Tables 1 and 2. Ground classification is improved by G_i* regardless of the window sizes. However, improvement in non-ground classification is not so obvious. Omission errors in ground classification decrease from the LMI-based 25-29% to the G_i*-based 16-20% (see Tables 1 and 2). On the other hand omission errors in non-ground classification decrease slightly from the LMI-based 28-35% to the G_i*-based 23-31%. Therefore it can be concluded that overall omission errors are higher than expected. This problem will be discussed in Section 5.

Commission errors in ground classification increase from the LMI-based 1-7% to the G_i* -based 10-12%, and commission errors in non-ground classification also increase from the LMI-based 2-7% to the G_i* -based 7-10%. Hence it is obvious that the LMI-based algorithm provides a more reliable result in terms of commission errors. From Tables 1 and 2, it can be seen that the least commission error in ground classification is obtained by using the window size of 100 m. In addition, the least commission error in non-ground classification is obtained by the window size of 150 m if the LMI-based is used (Table 1), and by 100 m in case of the G_i* -based (Table 2).

Table 1. Level of errors in rasters of ground and non-ground points.

Window Sizes (m)	LMI			
	Omission Errors (%)		Commission Errors (%)	
	GRD*	NGRD**	GRD	NGRD
100	29	28	1	3
150	25	31	4.8	2
200	28	35	7.4	7

*GRD: Ground Classification, **NGRD: Non-ground Classification

Table 2. Table 2.Level of errors in rasters of ground and non-ground points

Window Sizes (m)	G_i*			
	Omission Errors (%)		Commission Errors (%)	
	GRD*	NGRD**	GRD	NGRD
100	16	23	10	7.4
150	16	28	10	9.2
200	20	31	12	10

A significant reduction of omission errors in ground classification by the G_i* based algorithm can be realized by comparing the ground points extracted from the two proposed methods. The results show that G_i* with the 100-m window size provides the least omission error and this is also confirmed by the error calculation given in Table 2. One of the areas subject to a high level of omission errors in non-ground classification is a slant area. From a visual inspection, it is likely that the least omission error by LMI seems to be obtained by the 150-m window size, however, Table 1 indicates otherwise i.e. the least error comes actually from the 100-m window size. From another visual inspection, it is seen that the omitted points in the 200-m window size are clustered in the slant and complex areas but the omitted points in the 150-m window size are dispersed.

Tables 1and 2 represent that the commission error in non-ground classification is overall lower than that in ground classification, except the commission error in ground classification by LMI with the 100-m window size is the lowest. From the results, it can be concluded that the problematic areas of high commission errors are slant areas and object boundaries. Visual inspections of the errors demonstrate that the commission errors by both methods are lower if the 100-m window size is used. An interesting result is that the commission errors in non-ground classification are not affected much by the slope. In addition, the omission error for ground classification decreases to 23% for the LMI-based algorithm and to 15% for the G_i*-based algorithm when we combine (see Figure 3) the ground points extracted by 100-m, 150-m and 200-m window sizes. While the omission error reduces by combining the results from different window sizes, the commission error increases.

All in all, it is observed that, in the cluster of low values (G_i* < -1.65 or $|z_i|$ < -2.58 and p-value < 0.05), 93% of the points are ground points when the window size of 100 m is used. Larger windows tend to decrease this rate to 82.5% (for the 150-m window size) and 75.5% (for the 200-m window size). On the other hand, in the cluster of high values (G_i* > +1.65 or $|z_i|$ < -2.58 and p-value < 0.05), a high portion of the points are non-ground points: 99.9% for the window sizes of 200 m and 150 m, and 99.8% for the 100-m window size. Therefore it is reasonable to conclude that the window size of 100 m outperforms the other choices and the corresponding commission error is very small. However, it should be noted that a substantial amount of points still do not belong to either the low LMI clusters or the high LMI clusters, hence the omission error can increase.

5 Discussion

The main aim of this research was to apply LMI and G_i* to the lidar data classification and find one that outperforms the other. The results, however, indicate that the two algorithms are comparable to each other i.e. the G_i*-based algorithm produces lower omission errors but higher commission errors than the LMI-based does. In addition, it is observed that most of the commission errors in ground classification occurred in slope areas. This problem is also reported by Meng et al. [20] that slant areas are challenging for cluster-based classifiers. Therefore, a slope-based algorithm is suggested to reduce the commission errors.

It should be noted that the results of the proposed algorithms depend on window sizes and neighbours per lidar point (i.e. the lidar points within the given window size). In that sense, the study area for this research is very challenging because it contains high-rise buildings, large-area buildings, complex scenes and slant areas. Therefore the omission errors in ground classification were higher than expected. This problem can be minor if an accurate DEM can be generated from the classified ground points, provided small commission errors. That is, the LMI-based algorithm can be applied to the DEM generation, and then the G_i*-based algorithm can be applied to the non-ground classification.

It is noticed that the level of error is significantly influenced by the method of calculation. For example, point-wise error calculation decreases considerably when compared to rasterisation-based calculation. Moreover, it is shown that the low vegetation threshold for DEM generation affects both Type I and II errors [18]. Future work is to determine an optimal threshold to lower the level of omission and commission errors.

6 Concluding Remarks

It was shown in this paper that LMI and Gi* can be used effectively as the automatic classifiers of lidar points to ground and non-ground points. The test results from the two algorithms exhibit that each has advantages and disadvantages. The LMI-based algorithm provides lower-level commission errors, and the Gi* based algorithm produces lower-level omission errors. Therefore, the LMI-based algorithm is suitable for the DEM generation, and the Gi*-based algorithm is preferable for the feature extraction.

As for ground classification, slant areas are identified as the main source of the commission errors from both classifiers, and of the omission errors from the LMI-based classifier, regardless of the window sizes. However, the slant areas do not cause significant commission errors in non-ground classification. It is also observed that the commission errors in non-ground classification are dispersed, whereas the commission errors in ground classification are clustered. In plain areas, the commission errors occurred mainly on the boundaries of buildings and vegetation. It is suggested that the proposed algorithms with a moving window or an ad-hoc window size can reduce such commission errors.

References

[1] Pingel, T.J., K.C. Clarke, and W.A. McBride, An improved simple morphological filter for the terrain classification of airborne LIDAR data. *ISPRS Journal of Photogrammetry and Remote Sensing*, 77(0):21-30, 2013.

[2] Silván-Cárdenas, J.L. and L. Wang, A multi-resolution approach for filtering LiDAR altimetry data. *ISPRS Journal of Photogrammetry and Remote Sensing*, 61(1):11-22, 2006.

[3] Mongus, D. and B. Žalik, Parameter-free ground filtering of LiDAR data for automatic DTM generation. *ISPRS Journal of Photogrammetry and Remote Sensing*, 67(0):1-12, 2012.

[4] Li, Y., et al., A gradient-constrained morphological filtering algorithm for airborne LiDAR. *Optics & Laser Technology*, 54(0):288-296, 2013.

[5] Sithole, G. and G. Vosselman, Experimental comparison of filter algorithms for bare-Earth extraction from airborne laser scanning point clouds. *ISPRS Journal of Photogrammetry and Remote Sensing*, 59(1–2):85-101, 2004.

[6] Golany, G.S., Urban design morphology and thermal performance. *Atmospheric Environment*, 30(3):455-465, 1996.

[7] Talen, E., et al., LEED-ND as an urban metric. *Landscape and Urban Planning*, 119(0):20-34, 2013.

[8] Lam, N.S.-N., et al., An evaluation of fractal methods for characterizing image complexity. *Cartography and geographic information science*, 29(1):25-35, 2002.

[9] Emerson, C.W., N.S.-N. Lam, and D.A. Quattrochi, A comparison of local variance, fractal dimension and Moran's I as aids to multispectral image classification. *International journal of remote sensing*, 26(8):1575-1588, 2005.

[10] Su, W., et al., Textural and local spatial statistics for

the object -oriented classification of urban areas using high resolution imagery. *International journal of remote sensing*, 29(11):3105-3117, 2008.
[11] Mallinis, G., et al., Object-based classification using Quickbird imagery for delineating forest vegetation polygons in a Mediterranean test site. *ISPRS Journal of Photogrammetry & Remote Sensing*, 63:237-250, 2008.
[12] Roggero, M., Airborne laser scanning-clustering in raw data. *International Archives of Photogrammetry Remote Sensing and Spatial Information Sciences*, 34(3/W4):227-232, 2001.
[13] Lewin, S.S., Urban sustainability and urban form metrics. *Journal of Green Building*, 7(2):44-63, 2012.
[14] Zhang, P., Y. Hu, and H. He. The spatial pattern of building height in Tiexi District. In *2011 International Conference on Electric Technology and Civil Engineering (ICETCE),* 2011.
[15] Getis, A. and J.K. Ord, Local spatial statistics: an overview, in Spatial analysis: modelling in a GIS environment, P. Longly and M. Batty, Editors. 1996, Geoinformation international Cambrdge. p. 261-277.
[16] Zhang, K., et al., A progressive morphological filter for removing nonground measurements from airborne LIDAR data. *Geoscience and Remote Sensing, IEEE Transactions on*, 41(4):872-882, 2003.
[17] Ebdon, D., *Statistics in Geography*. Basil Blackwell, USA, 1985.
[18] Estornell, J., et al., Analysis of the factors affecting LiDAR DTM accuracy in a steep shrub area. *International Journal of Digital Earth*, 4(6):521-538, 2011.
[19] Getis, A. and J.K. Ord, The analysis of spatial association by use of distance statistics. *Geographical analysis*, 24(3):189-206, 1992.
[20] Meng, X., N. Currit, and K. Zhao, Ground Filtering Algorithms for Airborne LiDAR Data: A Review of Critical Issues. *Remote Sensing*, 2(3):833-860, 2010.